HHS Public Access

Author manuscript

Biochem J. Author manuscript; available in PMC 2017 May 27.

Published in final edited form as:

Biochem J. 2016 March 01; 473(5): 627–639. doi:10.1042/BJ20151150.

Role of Munc13-4 as a Ca^{2+}-dependent tether during platelet secretion

Michael C. Chicka[1,3], **Qiansheng Ren**[1,4], **David Richards**[2,5], **Lance M. Hellman**[1,6], **Jinchao Zhang**[1], **Michael G. Fried**[1], and **Sidney W. Whiteheart**[1,†]

[1]Department of Molecular and Cellular Biochemistry, University of Kentucky College of Medicine, Lexington, KY

[2]Department of Anesthesia, Cincinnati Children's Hospital and Medical Center, Cincinnati, OH

Abstract

The Munc13 family of exocytosis regulators has multiple Ca^{2+}-binding, C2 domains. Here, we probed the mechanism by which Munc13-4 regulates *in vitro* membrane fusion and platelet exocytosis. We show that Munc13-4 enhances *in vitro* SNARE-dependent, proteoliposome fusion in a Ca^{2+}- and phosphatidylserine (PS)-dependent manner that was independent of SNARE concentrations. Munc13-4-SNARE interactions, under the conditions used, were minimal in the absence or presence of Ca^{2+}. However, Munc13-4 was able to bind and cluster liposomes harboring PS in response to Ca^{2+}. Interestingly, Ca^{2+}-dependent liposome binding/clustering and enhancement of proteoliposome fusion required both Munc13-4 C2 domains, but only the Ca^{2+}-liganding aspartate residues of the C2B domain. Analytical ultracentrifugation measurements indicated that, in solution, Munc13-4 was a monomeric prolate ellipsoid with dimensions consistent with a molecule that could bridge two fusing membranes. To address the potential role of Munc13-4 as a tethering protein in platelets, we examined mepacrine-stained, dense granule mobility and secretion in platelets from wild-type and Munc13-4 null (*Unc13d*^{jinx}) mice. In the absence of Munc13-4, dense granules were highly mobile in both resting and stimulated platelets, and stimulation-dependent granule release was absent. These observations suggest that dense granules are stably docked in resting platelets awaiting stimulation and that Munc13-4 plays a vesicle-stabilizing or tethering role in resting platelets and also in activated platelets in response to Ca^{2+}. In summary, we show that Munc13-4 conveys Ca^{2+} sensitivity to platelet SNARE-mediated

[†]**To whom correspondence should be sent:** Sidney W. Whiteheart, Ph.D., Department of Molecular and Cellular Biochemistry, University of Kentucky College of Medicine, 741 South Limestone, BBSRB271, Lexington, KY 40536-0509, Tel.: 859-257-4882, Fax: 859-257-2283, whitehe@uky.edu.

[3]**Present Address:** PreventionGenetics, 3800 S. Business Park Ave., Marshfield, WI 54449, USA

[4]**Present Address:** Department of Protein Chemistry, Beijing Novo Nordisk Pharmaceuticals Science & Technology Co. Ltd, No.29 Life Science Park Road, Changping District, Beijing 102206, China

[5]**Present Address:** Department of Basic Pharmaceutical Sciences, School of Pharmacy, Husson University, 1 College Circle, Bangor, ME 04401, USA

[6]**Present Address:** Department of Chemistry and Biochemistry, University of Notre Dame, Harper Cancer Research Institute, 1234 Notre Dame Avenue, South Bend, IN 46617, USA

DISCLOSURE OF CONFLICTS OF INTEREST: The authors declare no competing financial interest.

AUTHORSHIP CONTRIBUTIONS: M.C.C. and Q.R. performed the experiments and J.Z. assisted, D.R. assisted in design and data analysis of the granule mobility studies. L.M.H and M.G.F. carried out the analytical centrifugation analysis. S.W.W. directed the research and with M.C.C. prepared the manuscript.

membrane fusion and reveal a potential mechanism by which Munc13-4 bridges and stabilizes apposing membranes destined for fusion. (246 words)

Keywords

exocytosis; platelets; Munc13-4; membrane fusion; C2 domains

INTRODUCTION

Platelets are “first responders” to vascular injury playing a key role in maintaining vascular homeostasis. Damage to endothelial cells exposes signaling molecules (*e.g.* collagen and von Willebrand factor (VWF)) that bind platelet surface receptors and initiate thrombosis and hemostasis. Upon activation, platelets adhere to sites of damage, undergo a series of shape changes, and release a range of molecules from three types of granule stores. Dense granules (~7 per platelet) contain small molecules such as adenosine 5’-diphosphate (ADP), adenosine triphosphate (ATP), serotonin, and calcium that are important for platelet activation and vasoconstriction (1). Alpha granules are the most abundant (~50 per platelet) and contain polypeptides such as VWF, fibrinogen, fibronectin, and platelet factor 4 (PF4), which are important for platelet adhesion and aggregation (2). Finally, lysosomes, which are few in number, contain acid hydrolases that could aid in clot remodeling (2). The importance of platelet cargo secretion is seen in granular storage pool deficiencies such as Hermansky Pudlak Syndrome (HPS) and Gray Platelet Syndrome (GPS), in which platelets lack either dense or α-granule content, respectively (3–6). Patients with HPS display increased bleeding times, pigmentation defects, and lung fibrosis whereas GPS is characterized by myelofibrosis and a range of bleeding defects (6). In contrast to these deficiencies, hyperactive platelet secretion causes spurious thrombosis and increased risk for heart attack and stroke (7–10).

Much like synaptic transmission, platelet granule secretion is triggered by a rise in intracellular calcium concentration $[Ca^{2+}]_i$. Also like synaptic transmission, secretion is catalyzed by *trans*-interactions between soluble NSF attachment protein receptors (SNAREs) residing on secretory vesicles/granules (v-SNAREs) and on the plasma/target membrane (t-SNAREs). Formation of a cognate SNARE complex bridges fusing membranes and drives fusion and cargo release (11, 12). Platelets contain a variety of v-SNAREs and t-SNAREs, but previous studies from our laboratory and others suggest that VAMP8 acts as a primary v-SNARE for granule secretion and heterodimer complexes comprising syntaxin-11 and SNAP-23 are key t-SNARE complexes (13–17). Recently, VAMP7 and Syntaxin 8 have been shown to also contribute to platelet exocytosis (18, 19). While SNARE proteins are the core membrane fusion machinery, a host of regulatory proteins affect the timing, location, and Ca^{2+}-sensitivity of secretion. Important regulators identified in platelets include members of the Sec1/Munc18 family, specifically Munc18b (20, 21), the small GTPase Rab27a (22), Tomosyn1/STXBP5 (23) and Munc13-4 (24–26). These proteins are thought to regulate vesicle “tethering” and “priming” prior to secretion, but their exact roles remain unclear. It is particularly interesting that little is known about the putative Ca^{2+}-sensor(s) required for platelet secretion and function.

In neuroendocrine cells, synaptotagmins act as Ca^{2+}-sensors for secretion (reviewed in (27)) through their two Ca^{2+}-binding C2 domains termed C2A and C2B. The C2 domains coordinate Ca^{2+}-dependent interactions with SNARE proteins and anionic phospholipids (*i.e.* phosphatidylserine, PS) (see (27)). Though synaptotagmin-like proteins (Slp1, 4) have been found in platelets (28, 29), a mechanistic understanding of their roles is incomplete. Munc13-4, also contains two C2 domains and appears to play a central role in Ca^{2+}-triggered secretion from a number of cells of the hematopoietic lineage (24, 26, 30–33). In neutrophils, Munc13-4 is present in cytosol and on various membranes, but upon stimulation, it concentrates onto membrane fractions in a Ca^{2+}-dependent manner (34). Recent reports showed that secretory vesicle motility decreases in neutrophils and RBL-2H3 mast cells just prior to stimulated secretion suggesting that vesicles are “corralled” or stabilized at specialized sites just prior to membrane fusion (35, 36). Importantly, this vesicle stabilization is lost either in the absence of Munc13-4, or when Munc13-4-Rab27a interactions are disrupted (35, 36). In platelets, dense granule secretion is abolished in the absence of Munc13-4 while α-granule and lysosomal secretion are attenuated (24, 26, 33). Ren *et al*. showed that the secretion defect in platelets lacking Munc13-4 could be rescued by adding recombinant Munc13-4 and Ca^{2+} to permeabilized platelets. Data from Ren *et al.* also showed that secretion was directly proportional to the amount of Munc13-4 added. These data revealed a putative Ca^{2+}-dependent role for Munc13-4 in platelets and identified Munc13-4 as a limiting factor, essential for platelet granule exocytosis (24). While clearly required, the molecular mechanism of Munc13-4 action remains unknown.

Here, we look directly at the Ca^{2+}-dependent role of Munc13-4 using an *in vitro* membrane fusion assay and real-time imaging of platelet dense granule secretion. We show that Munc13-4 conveys Ca^{2+}-sensitivity *directly* to *in vitro* membrane fusion mediated by platelet t-SNAREs and v-SNAREs. We demonstrate that Munc13-4 binds to the anionic phospholipid phosphatidylserine in a Ca^{2+}-dependent manner, but does not bind to platelet SNAREs in response to Ca^{2+}. We further show that Ca^{2+}-dependent Munc13-4-phospholipid interactions mediate vesicle aggregation in solution. These experiments mimic the vesicle-stabilizing role of Munc13-4 shown in other hematopoietic cells, but uniquely demonstrate that in the absence of other cellular factors, Ca^{2+}-Munc13-4 alone effectively stabilizes vesicles and stimulates SNARE-mediated membrane fusion. This is supported by our observations that mutating the C2 domain Ca^{2+}-ligands in Munc13-4 abolishes Ca^{2+}-dependent Munc13-4 action *in vitro*. Finally, using time-lapse, 3-dimensional fluorescence microscopy, we show that dense granule secretion is ablated in platelets lacking Munc13-4, thereby confirming results from our previous studies, and further show that dense granules in Munc13-4$^{-/-}$ platelets are highly mobile in comparison to dense granules in wild type platelets. Moreover, granule mobility increases in response to Ca^{2+}, suggesting that Munc13-4 plays a Ca^{2+}-independent and Ca^{2+}-dependent role in stabilizing vesicles prior to and during membrane fusion. These data show that Munc13-4 directly regulates Ca^{2+}-triggered, SNARE-mediated membrane fusion both *in vitro* and in platelets and highlight the importance of Munc13-4 action during membrane fusion and the final steps of granule secretion.

EXPERIMENTAL PROCEDURES

Plasmids and protein purification

DNAs encoding the human Munc13-4 open reading frame (amino acids 1-1090) and all mutants were inserted into the pENTR/D-Topo vector (Invitrogen, Carlsbad, CA) and subcloned into the pDEST10 vector (Invitrogen). The pDEST10-Munc13-4 or mutant plasmids were then used to transform DH10Bac cells (Invitrogen) and the positive Bacmid was isolated to infect Sf9 cells to produce baculovirus. Infected Sf9 cells were collected 72 hr later and His_6-tagged, recombinant proteins were first purified by Ni^{2+}-NTA agarose chromatography using standard procedures followed by gel-filtration chromatography on Superose 6 (GE Healthcare, Piscataway, NJ; in 25 mM HEPES/KOH pH 7.4, 150 mM KCl, 2 mM β-mercaptoethanol). The full-length expression construct was modified by truncation to create ΔC2A (amino acids 274-1090) and ΔC2B (amino acids 1-910) or by site-directed mutagenesis using the QuickChange kit (Stratagene, Santa Clara, CA). The following mutations were created to eliminate calcium binding to the C2 domains: for C2A: D127N, D133N, D206N, D208N and D241N; for C2B: D941N, D947N, D1005N, D1007N, and D1013N. The protein preparations were >90% pure as evaluated by SDS-PAGE and Coomassie Blue staining (data not shown).

DNA encoding the open reading frames of rat Syntaxin 2 (amino acids 1-290; provided by J.M. Edwardson, University of Cambridge) and SNAP-23 (provided by E. R. Chapman, University of Wisconsin) was inserted into the pRSFDuet expression vector (Merck Millipore, Billerica, MA). All cDNA was checked for variants and corrected to wild-type sequence if necessary. DNA encoding mouse VAMP8 (amino acids 1-101; provided by Wan Jin Hong, Institute of Molecular and Cell Biology, Singapore) was inserted into the pPROEX expression vector (Life Technologies, Grand Island, NY). A stop codon was engineered into the pPROEX VAMP8 construct prior to the nucleotides encoding the transmembrane domain in order to express the cytoplasmic domain of VAMP8 (cdV8, amino acids 1-75). His_6-tagged, recombinant t-SNARE heterodimers comprising Syntaxin 2 and SNAP-23 proteins and recombinant v-SNARE VAMP8 (or cdV8) protein were expressed and purified by Ni^{2+}-NTA agarose chromatography as described (37). All t- and v-SNARE proteins were washed in buffer containing nucleases and high salt to remove bacterial contaminants and eluted in 25 mM HEPES, pH 7.4, 200 mM KCl, 1 mM DTT.

Preparation of protein free and SNARE-bearing vesicles

All lipids were obtained from Avanti Polar Lipids (Alabaster, AL). Reconstitution of t-SNARE vesicles harboring Syntaxin 2 + SNAP-23 heterodimers and of v-SNARE vesicles harboring VAMP8 was carried out as described (37, 38). t-SNAREs were reconstituted using a lipid mix comprising 30% (mol/mol) 1-palmitoyl-2-oleoyl-phosphatidyl-ethanolamine (PE), 40% 1-palmitoyl, 2-oleoyl phosphatidylcholine (PC), and 30% 1,2-dioleoyl phosphatidylserine (PS). v-SNAREs were reconstituted using a lipid mix comprising 27% PE, 40% PC, 30% PS, 1.5% *N*-(7-nitro-2-1,3-benzoxadiazol-4-yl)-1,2-dipalmitoyl phosphatidyl-ethanolamine (NBD-PE, FRET donor) and 1.5% *N*-(lissamine rhodamine B sulfonyl)-1,2-dipalmitoyl phosphatidylethanolamine (Rhodamine-PE, FRET acceptor). Protein free vesicles were reconstituted similarly with omission of protein. PC was

substituted for PS when PS was omitted from vesicles. Protein free vesicles of a fixed diameter were reconstituted using standard lipid extrusion through 100 nm pore filters and a LIPEX 1.5–10 ml extruder (Northern Lipids Inc., Burnaby, BC, Canada).

Flotation assays

Flotation assays were carried out as described previously (39). Briefly, Munc13-4 protein was mixed with t-SNARE or v-SNARE vesicles lacking PS or with protein free vesicles with PS in reaction buffer (25 mM HEPES, pH 7.4, 200 mM KCl, 1 mM DTT) and a final volume of 150 µl. Reactions were carried out in 0.2 mM EGTA or 1 mM Ca^{2+}. Samples were incubated at room temperature for 1 hr with shaking, mixed with an equal volume of 80% Accudenz media (Accurate Chemical and Scientific, Corp., Westbury, NY) in reaction buffer, and layered with 35%, 30%, and 0% Accudenz in reaction buffer containing either 0.2 mM EGTA or 1 mM Ca^{2+}. Samples were centrifuged at 280,000 × g for 2.5 hr at 4°C. Vesicles were collected from the 0%/30% Accudenz interface and equal volumes from each reaction were analyzed by SDS-PAGE and stained with Coomassie Blue. Standards indicate the electrophoretic mobility of the proteins.

Reconstituted membrane fusion assays

Fusion assays were carried out as described (38). Briefly, each 75 µl reaction consisted of 5 µl purified t-SNARE vesicles and 5 µl of purified, NBD- and Rhodamine-PE–labeled v-SNARE vesicles plus 0.2 mM EGTA in 25 mM HEPES, pH 7.4, 200 mM KCl, 1 mM DTT. All components of the fusion reaction were prewarmed to 37 °C for 10 min separately before being mixed together at $t = 0$ min. Fusion was monitored as an increase in NBD fluorescence using a Bio-TEK FLx800 Microplate Fluorescence Reader and KC4 software (BioTek Instruments, Inc., Winooski, VT) with data acquisition every 30 sec during rapid Ca^{2+}-induced fusion, and every 1.5–2.0 min during slower phases. After 60 min, 0.5% (w/v) n-dodecylmaltoside (Roche Applied Science, Indianapolis, IN) was added to maximally dequench the NBD fluorescence, yielding a maximum fluorescence signal. Raw fluorescence was converted to percentage of the maximum fluorescence as described (37). When included, Ca^{2+} was added to reactions manually around $t = 20$ min by pausing the microplate reader during Ca^{2+} addition to the appropriate wells, and restarting the microplate reader after the final Ca^{2+} addition.

Dynamic light scattering measurements

Protein-free liposomes were extruded using a 100 nm pore (see above). Liposome aggregation was used as a metric for granule tethering. Briefly, wild-type Munc13-4 or mutant Munc13-4 was mixed with liposomes having a composition of: 70% PC/30% PE or 40% PC/30% PE/30% PS. Reactions contained 0.2 mM EGTA in reaction buffer and were analyzed in a DynaPro 99 instrument (ProteinSolutions, Inc., Charlottesville, VA) with a scattering angle of 90° for ~ 5 min in order to obtain baseline levels of aggregation. After 5 min, Ca^{2+} (final concentration of 1 mM) was added as indicated and aggregation was measured again for ~ 5 min. Data were analyzed with Dynamics Software (Version 5.19.06). An increase in particle size was taken as evidence of liposome aggregation. Since no SNAREs are present, the liposomes do not fuse.

Analytical ultracentrifugation

Sedimentation velocity experiments were performed in a Beckman XL-A analytical ultracentrifuge (Beckman, Fullerton, CA) using an An-60Ti rotor operated at 40,000 rpm and 4°C. Samples were run in 25 mM HEPES (pH 7.4), 150 mM KCl, 2 mM β-mercaptoethanol with either 1 mM of added $CaCl_2$ or EGTA. Data were fit with numerical solutions of the Lamm equation, implemented in the SEDFIT program (40, 41). Experimental *s* values ($s_{T,B}$) were converted to standard $s_{20,w}$ conditions using Equation 1 (42).

$$s_{20,w} = s_{T,B} \frac{(1 - \overline{\nu}\rho_{20,w})\left(\eta_{T,B}\right)}{(1 - \overline{\nu}\rho_{T,B})(\eta_{20,w})} \quad (1)$$

Here $\overline{\nu}$ is the partial specific volume (0.7385 ml/g) calculated from sequence composition using the SEDNTERP program (42), ρ is the buffer density (measured using a Mettler density meter, Mettler Toledo, Columbus, OH) and η the buffer viscosity, calculated from tabulated values using SEDNTERP.

Mice and genotyping

The genotype of each mouse was determined by PCR using DNA from a tail tip biopsy as described (24). All animal work was approved by the University of Kentucky IACUC.

Platelet preparation

Mice were euthanatized by CO_2 inhalation. Blood was collected from the right ventricle and was mixed with sodium citrate to a final concentration 0.38%. The citrated blood was mixed with an equal volume of PBS, pH 7.4. Platelet rich plasma (PRP) was prepared by centrifugation at 250×g for 10 min. After adding 10 ng/mL prostaglandin I_2 (Sigma) for 5 min, the PRP was centrifuged at 500×g for 15 min and the platelet pellet was gently resuspended in HEPES/Tyrode's Buffer (10 mM HEPES/NaOH, pH 7.4, 5.56 mM glucose, 137 mM NaCl, 12 mM $NaHCO_3$, 2.7 mM KCl, 0.36 mM NaH_2PO_4, 1 mM $MgCl_2$) in the presence of 3 μg/mL of apyrase (Sigma) and 1 mM EGTA.

Time-lapse, three-dimensional (3D) fluorescence microscopy

Dense granules in wild-type or *Unc13d*^{Jinx} platelets mice were labeled with mepacrine (1 μM, 15 min, at 37°C, Sigma, St. Louis, MO) and imaged in suspension by 3D fluorescence microscopy. Imaging was carried out on an Olympus ix80 inverted microscope with integrated high precision focus drive. Fluorescence excitation was provided by a rapid switching DG4 light source (Sutter Instruments, Novato, CA) attached by liquid light guide. The cooled CCD camera was a Hammamatsu ORCA R2, communicating to the host computer *via* firewire interface (Hammamatsu, SZK, Japan). The objective used for 3D acquisition was an APO N 65x 1.49 NA objective optimized for fluorescence (Olympus, Shinjuku, Tokyo, Japan). 3D stacks were taken with 5–6 sections 400 nm apart, at a frequency of 0.5Hz per 3D time point. Image analysis was done with Slidebook 5 software (Intelligent Imaging Innovations, Denver, CO). The rates of dense granule release were

assessed by measuring the loss of fluorescence following stimulation with 0.7 mM Ca^{2+} and A23187 (1 μM, Sigma). To examine granule movement, individual granules were selected from fields, based on the following criteria: (1) granule fluorescence is constant during the observation period (not released); (2) the platelet remains static in the field of view; and (3) the platelet does not impinge on the upper or lower boundaries of the 3D stack. Particle tracking was done with Slidebook's particle tracking tool, and movement was based on the center of intensity for each granule. We plotted MSD (mean square displacement) against time, as according to the equation MSD (mean square displacement) = $6Dt$, the slope is proportional to the diffusion coefficient (D). To stimulate platelets, the ionophore A23187 was used because it results in a more even activation of platelets in a viewing field and is less subject to diffusional effects.

RESULTS

Munc13-4 stimulates membrane fusion in response to Ca^{2+}

In hematopoietic cells, little is known about the sequence of molecular events that drive granule/plasma membrane fusion during Ca^{2+}-triggered secretion. In some systems, fusion competent granules appear to be "docked" at fusion sites under resting Ca^{2+} concentrations and rapidly fuse with the plasma membrane in response to a rise in intracellular Ca^{2+}. In platelets, upon Ca^{2+} activation, the serotonin secretion time course is rapid suggesting that the membrane fusion machinery is capable of sensing Ca^{2+} and quickly converting that signal into granule secretion (43, 44). We recapitulated Ca^{2+}-dependent granule secretion using an *in vitro* membrane fusion assay comprising lipids, platelet SNAREs, and Munc13-4 (Figure 1A). The v-SNARE VAMP8 was reconstituted into one population of vesicles that contained membrane-anchored fluorescence energy transfer (FRET) donor-acceptor pairs. The t-SNARE heterodimer comprising syntaxin 2 and SNAP-23 was reconstituted into unlabeled vesicles (Figure 1A). When combined at 37°C, fusion between the two vesicle populations leads to dilution of the FRET pair from bilayer mixing of the labeled and unlabeled vesicles. This dilution yields an increase in the donor fluorescence intensity over time and thereby serves as a metric of membrane fusion (Figure 1A) (45). Figure 1B shows reconstituted SNARE-mediated membrane fusion. Addition of excess amounts of the cytoplasmic domain of VAMP8 (cdV8) saturates the t-SNAREs, inhibits vesicle-bound t-SNARE/v-SNARE interactions, and consequently inhibits membrane fusion. The cdV8 control therefore demonstrates that the observed fusion is SNARE-dependent. Though syntaxin 11 is the dominant syntaxin t-SNARE for platelet exocytosis (17), syntaxin 2 was used as a surrogate. Syntaxin 11 lacks a transmembrane domain and is associated with membranes via thioester-linked acyl groups (46). We have yet to produce sufficient acylated syntaxin 11 for proteoliposome fusion assays (Zhang *et al.* unpublished).

Increasing amounts of purified Munc13-4 protein were added to the proteoliposome fusion reactions and after 20 min, Ca^{2+} (1 mM) was added. Ca^{2+} addition had only a limited effect on SNARE-mediated fusion in the absence of Munc13-4. In contrast, addition of Ca^{2+} to reactions containing Munc13-4 resulted in a dramatic increase in membrane fusion that was dependent on the amount of added Munc13-4 (Figure 1B–D). As observed with other C2 domain containing proteins (39), omission of phosphatidylserine (PS) from SNARE-bearing

vesicles had little effect on SNARE-mediated membrane fusion, but abolished the ability of Munc13-4 to stimulate fusion in response to Ca^{2+} (Figure 3A).

Substituting wild type Munc13-4 with a mutated Munc13-4, in which the Ca^{2+}-coordinating aspartates in both the C2A and C2B domains were converted to asparagines, resulted in a loss of Ca^{2+}-dependent membrane fusion (Figure 1E). Truncated versions of Munc13-4 that lacked either the C2A domain or the C2B domain were also unable to stimulate SNARE-mediated membrane fusion in response to Ca^{2+} (Figure 1F). Interestingly, in the context of full-length Munc13-4, only mutations of the Ca^{2+}-ligands of C2B ablated Ca^{2+}-dependent, Munc13-4-stimulated membrane fusion;Munc13-4 retained Ca^{2+}-dependent activity when only the Ca^{2+}-ligands in C2A were altered (Figure 1G). These results suggest that the C2B domain is required for Ca^{2+}-dependent Munc13-4 activity, but also hint at a cryptic Ca^{2+}-independent requirement for the C2A domain. Taken as a whole, these data demonstrate that Munc13-4 can act as a Ca^{2+}-sensor for platelet SNARE-mediated membrane fusion *in vitro* and that both the C2A and C2B domains are important.

Characterization of Ca^{2+}-dependent Munc13-4 interactions

C2 domains (*e.g.* in phospholipase A2, protein kinase C, and synaptotagmin) serve as Ca^{2+}-dependent phospholipid-binding moieties (47). In some cases (*i.e.*, synaptotagmin (27)), C2 domains coordinate Ca^{2+}-dependent interactions with SNAREs. To determine the relative importance of phospholipids and/or SNAREs to the Ca^{2+}-dependent, Munc13-4-stimulated membrane fusion, we employed a co-floatation assay (Figure 2A) (37, 38). Purified Munc13-4 was incubated with SNARE-bearing or protein-free liposomes in the absence or presence of Ca^{2+}. Reactions were layered on a density gradient and vesicles were purified by "floating" them to the top of the gradient *via* centrifugation. For this experiment the SNARE-bearing vesicles contained only phosphatidylcholine (PC) and phosphatidyl-ethanolamine (PE); neutral phospholipids that do not bind C2 domains (48). Thus, co-floatation of Munc13-4 with SNARE-bearing vesicles is a true metric of SNARE-Munc13-4 binding. To monitor Munc13-4 lipid interactions, the protein free vesicles contained phosphatidylserine (PS), a known Ca^{2+}-dependent effector of C2 domains(48) and a component of the t-SNARE and v-SNARE proteoliposomes used in the fusion assays in Figure 1.

In Figure 2B, only low levels of Munc13-4 were found associated with t-SNARE and v-SNARE vesicles in both the absence and presence of Ca^{2+}. These data suggest that Munc13-4 binds SNAREs to some extent, but under the conditions tested, does not show a robust increase in SNARE binding in response to Ca^{2+}. Conversely, Munc13-4 binding to protein-free vesicles containing PS dramatically increased in response to Ca^{2+}. Since *trans* SNARE complexes catalyze membrane fusion in a Ca^{2+}-independent manner (11, 49), these data suggest that the Ca^{2+}-dependent Munc13-4-phospholipid binding is a key part of the Munc13-4-stimulated, SNARE-mediated membrane fusion observed in Figure 1.

To explore further the role of Munc13-4-PS binding we altered the percentage of PS in the SNARE bearing vesicles, while keeping the SNARE copy number constant. If the protein-lipid interaction is truly important then the concentration of PS should directly correlate with the ability of Munc13-4 to stimulate membrane fusion in response to Ca^{2+}. As shown in

Figure 3A, the level of membrane fusion between v-SNARE and t-SNARE vesicles alone was not significantly affected by altering the amount of PS over a range of 15–30%. Munc13-4 did not stimulate fusion appreciably when vesicles contained only 15% or 20% PS. Increasing PS to 25% and then to 30% greatly enhanced Munc13-4's ability to stimulate fusion. We note that it was difficult to obtain vesicles with PS percentages higher than 30% because, in our hands, the higher concentrations of PS caused phospholipid precipitation during reconstitution.

To investigate the importance of Ca^{2+}-dependent, Munc13-4 -PS interactions in the fusion assay, we performed a series of reciprocal experiments in which the SNARE copy number in vesicles was altered while the PS concentration was kept constant. It was shown previously that altering the copy number of SNAREs on vesicles used in the reconstituted membrane fusion assay directly affected the ability synaptotagmin, another C2 domain-containing, Ca^{2+}-dependent regulator of membrane fusion, to stimulate membrane fusion (37). The experiments in Tucker *et al.* demonstrated that synaptotagmin acts, at least in part, through direct Ca^{2+}-dependent SNARE interactions (37). Applying the same principle, we reasoned that if Ca^{2+}-dependent, Munc13-4/SNARE interactions are important for Munc13-4 stimulated fusion, then altering the copy number of either v-SNAREs or t-SNAREs, while keeping the PS and Munc13-4 concentrations constant, should also correspondingly affect fold-stimulation above fusion obtained between v-SNARE and t-SNARE vesicles alone. In Figure 3B and C, increasing the copy number of v-SNAREs in vesicles, while keeping the copy number of t-SNAREs constant, did not affect the fold stimulation for a given concentration of Munc13-4. A similar result was seen when changing the copy number of t-SNAREs in vesicles while keeping the copy number of v-SNAREs constant (Figure 3C right panel). These data reveal that the dominant factor affecting Munc13-4's enhancement of membrane fusion is the PS concentration and not the SNARE concentration.

Munc13-4 clusters vesicles in a Ca^{2+}-dependent manner

Given the apparent importance of Munc13-4 PS interactions, the next series of experiments sought to probe the mechanism of how Ca^{2+}-dependent, Munc13-4-PS interactions could stimulate membrane fusion. It was suggested that Munc13-4 serves as a "tether" that stabilizes secretory vesicles prior to fusion with the plasma membrane (35, 36). Whether this function is Ca^{2+}-dependent, lipid-dependent or both, remains unclear. If Munc13-4 can tether secretory vesicles to the plasma membrane in response to Ca^{2+}, then in the reconstituted system, we would expect SNARE-free vesicles to form large grape-like clusters in the presence of Munc13-4 and Ca^{2+}. Using protein-free liposomes, we directly tested this using dynamic light scattering to measure the size of clusters formed in the absence or presence of Ca^{2+} and Munc13-4. We reasoned that in the absence of Ca^{2+}/Munc13-4, vesicles would be monodispersed in solution and of uniform size. If Munc13-4 is a tethering factor, in the presence of Ca^{2+}, the distribution of particle sizes in solution would shift to higher order species.

From the histograms in Figure 4A, in the absence of Munc13-4 and Ca^{2+}, vesicles in solution are distributed unequally among two populations—a small population with a size centered around 10 nm, and the vast majority of vesicles in a population centered around 90

nm, consistent with the extruder size used (left panel). The size distribution remained unchanged when Ca^{2+} was added to the reactions. The same was true when Munc13-4 was added to vesicles lacking the anionic phospholipid PS (Figure 4A middle panel). In contrast, when Munc13-4 and Ca^{2+} were added to vesicles containing PS, large vesicle aggregates formed in solution with a size centered around 10,000 nm, representing the detection limits of our instrument. These data are quantitatively represented in Figure 4B. We note that limiting amounts of Munc13-4 were used for this experiment because Munc13-4 in excess clusters essentially all of the vesicles in solution causing them to precipitate (data not shown). This phenomenon likely explains why increasing Munc13-4 concentrations above a certain threshold in the fusion reaction resulted in decreased membrane fusion (Figure 1B). We repeated the vesicle clustering experiments using the Ca^{2+}-ligand mutants described in Figure 1. The results mimicked those of the fusion reaction; Munc13-4 failed to cluster vesicles in response to Ca^{2+} when the aspartates were mutated to asparagines either in both the C2A and C2B domains or in the C2B domain alone (Figure 4C). Mutating the Ca^{2+}-ligands in the C2A domain alone did not affect the ability of Ca^{2+}-Munc13-4 to aggregate vesicles. These data suggest that clustering vesicles, *i.e.* "tethering" vesicles destined for fusion, is a major function of Ca^{2+}-Munc13-4 in the reconstituted system; however, these data do not rule out the possibility that Munc13-4 is also "doing work" on membranes during fusion (*e.g.* bending or destabilizing lipid bilayers of apposed membranes).

Hydrodynamic properties

The ability of Munc13-4 to aggregate liposomes in a Ca^{2+}- and PS-dependent manner raised the possibility that it might bridge two membranes. We examined the shape and oligomeric state of the protein by analytical ultracentrifugation in the presence or absence of Ca^{2+}, to determine if its structure provides clues to its function. The c(s) spectra of $s_{20,w}$ values, calculated with SEDFIT, are given in Figure 5. Our Munc13-4 preparations sedimented as single dominant species with $s_{20,w}$ ~5×10^{-13} s, with minor components at lower and higher s-values. Parallel analysis of c(M) distributions returned M_r = 118,285 ± 14,205 (mole fraction = 0.705) in the presence of Ca^{2+} and M_r = 112,464 ± 12,743 (mole fraction = 0.66) in the presence of EGTA. These values are consistent with the monomer molecular weight M_r = 107,742 calculated from the sequence of the recombinant protein. The program SEDNTERP (42) was used to calculate frictional ratios from observed $s_{20,w}$ values, returning f/f_0 = 1.58 ± 0.12 in EGTA buffer and 1.56 ± 0.11 in Ca^{2+} buffer, respectively. These values deviate from f/f_0 ~1.2, expected for hydrated, spherically-symmetrical globular proteins (50, 51). Modeling the protein as a prolate ellipsoid, with hydration of 0.3g/g-protein, typical for water-soluble proteins (52, 53), returned an axial ratio $\boldsymbol{a/b}$ = 7.35 ± 1.1, a semi-major radius $\boldsymbol{a}$ = 13.14 ± 0.65 nm and semi-minor radius $\boldsymbol{b}$ =1.82 ± 0.07 nm (Figure 5, inset). Thus the major axis of these molecules appears to be long enough ($2\boldsymbol{a}$ ~ 26 nm) to allow Munc13-4 to bridge between vesicle and plasma membranes to facilitate docking.

Platelet granule motility increases in response to Ca^{2+} in the absence of Munc13-4

Our *in vitro* data suggest that Munc13-4 could be a tethering factor, positioning secretory granules and bridging the two fusing membranes. Thus, Munc13-4 might be expected to link granules to potential fusion sites, *in vivo*, and thereby its deletion would be expected to affect granule distribution and stability. To address this in platelets, we monitored dense

granule secretion from control platelets and those lacking Munc13-4 (*Unc13d*^{Jinx} platelets (24)) using time-lapse, 3-dimensional fluorescence microscopy. It is well established that secretion from platelet dense granules is nearly abolished in the absence of Munc13-4 (24, 26, 33). The absolute requirement of Munc13-4 for dense granule secretion provided an ideal scenario for studying the role of Munc13-4 during secretion. By using mepacrine to fluorescently label platelet dense granules (54), we were able to monitor the kinetics of platelet dense granule secretion and to track granule motion both before and during activation with the ionophore, A23187, and Ca^{2+}.

We first compared dense granule secretion between control platelets and *Unc13d*^{Jinx} platelets by recording whole platelet fluorescence loss in response to activation. Figure 6A shows fields of either control or *Unc13d*^{Jinx} platelets, pre- and post-activation. The fluorescent puncta in the images represent dense granules loaded with mepacrine. It is clear that the number of puncta decreases in response to Ca^{2+}/A23187 in the control platelets but not in the *Unc13d*^{Jinx} platelets. Figure 6B highlights this observation by displaying images of two control platelets at different times after activation; by t=51 sec nearly all of the puncta, *i.e.* granules, are gone. The mean-relative-fluorescence versus time was plotted for control and *Unc13d*^{Jinx} platelets in Figure 6C. Secretion from control platelets is nearly complete within the first 10 sec following activation. In stark contrast, almost no loss of fluorescence occurred in *Unc13d*^{Jinx} platelets after 2 min. These data support previous findings that almost no dense granule secretion occurs in the absence of Munc13-4 (24, 26, 33).

We sought to determine whether the lack of dense granule secretion in *Unc13d*^{Jinx} platelets correlated with a lack of vesicle stabilization prior to granule-plasma membrane fusion and whether this stabilization had both Ca^{2+}-independent and Ca^{2+}-dependent components. We tracked individual granules in control and *Unc13d*^{Jinx} platelets *via* their center of intensity in three dimensions and plotted the mean-squared displacement (MSD) versus time. As shown in Figure 6D, even prior to stimulation, dense granules in control platelets are essentially motionless ($D = 31.7 \times 10^{-6}$ μm^3/s) whereas dense granules in *Unc13d*^{Jinx} platelets are highly mobile (D=0.002 μm^3/s). These data suggest Munc13-4 is required for a Ca^{2+}-independent vesicle stabilization step prior to secretion. Upon activation, dense granules in control platelets show little additional movement which is attributed largely to the fast rate at which they secrete their content. In contrast, the mobility of dense granules in *Unc13d*^{Jinx} platelets increases in response to Ca^{2+} suggesting that Munc13-4 is also required for a Ca^{2+}-dependent vesicle stabilization step prior to secretion. These data reveal that Munc13-4 plays a distinct Ca^{2+}-dependent role in vesicle stabilization that is required for platelet granule secretion.

DISCUSSION

In this manuscript, we probed the mechanisms by which Munc13-4 mediates membrane fusion and platelet exocytosis. We show that Munc13-4 enhanced SNARE-mediated, proteoliposome fusion in a Ca^{2+}- and PS-dependent manner that was not directly dependent on SNARE concentration. The fusion enhancement was dependent on the two C2 domains of Munc13-4 but required only the Ca^{2+}-liganding ability of the C2B aspartate residues.

Munc13-4 showed minimal binding to proteoliposomes containing SNAREs unless both PS and Ca^{2+} were present. Additionally, Munc13-4 caused the clustering of protein-free liposomes when Ca^{2+} and PS were included. This clustering activity again required specifically only the Ca^{2+}-liganding aspartate residues of C2B. Our data suggest that Munc13-4 can tether two lipid bilayers together in a manner that is both PS- and Ca^{2+}-dependent and that this tethering enhances the formation of fusogenic SNARE complexes. To understand the potential *in vivo* function of Munc13-4, we examined dense granule mobility and secretion in platelets from wild-type and *Unc13d*^{Jinx} mice. In the absence of Munc13-4 the granules were highly mobile in both resting and stimulated states and granule content was not secreted. These data yield new insights into platelet cell biology and activation. First they imply that mepacrine-stained dense granules are “docked” in the resting platelet awaiting stimulation, which may account for the rapidity of dense granule cargo release (44). Second they show that Munc13-4 plays a tethering role not only in activated platelets but also in resting platelets where Ca^{2+} levels are low.

SNAREs and Munc13-4 are required for platelet granule secretion (13–16, 18, 19, 24, 26), but little is known about the step-by-step order of events that culminate in Ca^{2+}-activated fusion of granules with the plasma membrane. Previous work from our lab showed that platelet dense granule secretion is ablated in the absence of Munc13-4 while α-granule and lysosomal secretion persist at attenuated rates (24). Thus, Munc13-4 is explicitly required for dense granule secretion. The data, presented here, suggest that dense granules reside in a docked/tethered state, close to the final stages of secretion. This heightened state of “readiness” requires Munc13-4 and allows dense granules to respond to a Ca^{2+}-trigger more rapidly than other platelet granule stores. Consistently, dense granule content is released more rapidly than is the content from α-granules or lysosomes (44). The rapid release of such molecules as ADP is critical for successful thrombosis and appears to constitute a feedback, paracrine factor for complete activation of α-granules and lysosome release (25, 26, 55, 56). Our finding that Munc13-4 is required for immobilizing dense granules offers new insights into the mechanisms of dense granule exocytosis and suggests that they exist in a “docked/tethered” state that is poised for release. This mechanism appears to be similarly used for lytic granules in cytotoxic T lymphocytes were loss of Munc13s increases granule mobility (57). Our data also account for the robust bleeding and hemostasis defect observed in the *Unc13d*^{Jinx} mice that lack the protein (24, 26, 58, 59) and are congruent with the phenotype observed in humans harboring mutations in *UNC13D*, the human homologue of Munc13-4 (60, 61). We addressed the role of Munc13-4 in response to Ca^{2+}, and in doing so revealed a role for Munc13-4 in unstimulated platelets. Future studies of Munc13-4 in resting conditions are required to shed light on this role of Munc13-4.

Reconstituted liposomes are an established tool for studying SNAREs and regulatory proteins involved in membrane fusion (11, 49). This system allowed us to analyze the role of Munc13-4 and its C2 domains in the final stages of granule secretion involving fusion between the vesicle membrane and the plasma membrane. We showed that Munc13-4 enhances SNARE-dependent, vesicle fusion in a Ca^{2+}-dependent manner that was specifically dependent upon Munc13-4 – liposome interactions and the Ca^{2+}-liganding aspartates of the C2B domain (Figure 1). The extent of fusion enhancement was independent of SNARE density and correlated with the amount of PS in the liposomes. We were unable

to detect a SNARE requirement for the Munc13-4-liposome association under the conditions we used in our assays employing t-SNARE complexes comprising syntaxin 2 and SNAP-23. This differs from Boswell *et al.* (62) who reported Ca^{2+}-independent interactions between Munc13-4 and four different, syntaxins (1, 2, 4 and 11) using GST-cytoplasmic domain fusion proteins, and Ca^{2+}-dependent interactions between Munc13-4 and liposome-embedded t-SNAREs comprising syntaxin 1 and SNAP-25. Perhaps the differences between our observations and those in Boswell *et al.* reflect innate preferences in Munc13-4 binding among different t-SNARE pairs in response to Ca^{2+}. Detailed SNARE-specificity studies are needed to clarify this. However, it should be noted that we were also unable to detect Munc13-4/syntaxin interactions by co-immunoprecipitation from platelet extracts, though Rab27/Munc13-4 interactions were readily detected (data not shown). Protein-free liposome aggregation can be a metric of granule/plasma membrane tethering prior to fusion. Consistent with our fusion data, both C2 domains were important for liposome aggregation as were the Ca^{2+}-liganding aspartates of C2B. Aggregation, like SNARE-mediated fusion, was dependent on Ca^{2+} and PS. Similarly, Boswell *et al.* (62) did show that PS was a required component for Munc13-4 liposome binding, however, in contrast to Boswell *et al.* our studies suggest that Munc13-4/SNARE interactions are not likely a primary requirement for the Ca^{2+}-dependent role of Munc13-4. Taken together, our data suggest that the ability of Munc13-4 to interact with acidic phospholipids in a Ca^{2+}-dependent manner is central to its role in tethering membranes and promoting SNARE-dependent fusion. Our data demonstrate directly that Munc13-4 helps juxtapose apposing membranes to stimulate membrane fusion in response to Ca^{2+}.

Our *in vitro* experiments recapitulate some of the steps just upstream of membrane fusion, *i.e.*, tethering. Neither fusion enhancement nor aggregation required Rab27 under the conditions used, though we did not test whether the Rab augmented either. From studies of knockout mice and biochemical analyses, Munc13-4 and Rab27 interact and are both important for platelet exocytosis (22, 24, 26, 63). In platelets, the ΔC2B mutant fails to rescue secretion from permeabilized *Unc13d*^{Jinx} platelets (24, 62). This mutant contains the Rab27a/b-binding site (amino acids 280-285 (35)) therefore this N-terminal region of Munc13-4 interacts with lipids, small-GTP binding proteins, and perhaps with other proteins important for exocytosis. These interactions, in the absence of the Ca^{2+}-dependent functions of C2B, are insufficient for platelet secretion suggesting a heterobifunctional mechanism for Munc13-4. The positioning of C2 domains at either end of Munc13-4 indicates that Munc13-4 could bridge two fusing membranes and thus facilitate tethering and SNARE-mediated fusion. Our AUC analysis showed that, in solution, monomeric Munc13-4 was an elongated, prolate ellipsoid with a semi-major axis length of 26 nm, which is sufficient to span between two membranes that are linked by SNAREs. Both C2 domains are important, but only one requires calcium-binding for function. The C2A-containing, ΔC2B mutant inhibits secretion from permeabilized platelets (24) and only one C2 domain (C2B) must bind Ca^{2+}; therefore, it seems plausible that the two C2 domains play distinct roles. This is often the case with other C2 domain containing proteins like synaptotagmins (see discussion below). Given that Rab27 is likely to be present on granules, one could envision that the Ca^{2+}-binding C2B domain is interacting with the plasma membrane and promoting SNARE mediated fusion in response to Ca^{2+}. The Rab27 interaction is not essential in our

reconstituted assay systems since Munc13-4 alone can interact with PS-containing liposomes and does not require a Rab27-dependent targeting to specific membranes (*i.e.*, granules). Previous reports showed that individual domains (*i.e.* MHD or C_2A) of a different Munc13 protein, Munc13-1, can dimerize (64, 65) or hetero-dimerize with fragments of α-RIM (65). These studies used purified domains of Munc13-1 comprising only portions of the whole protein; thus, it is difficult to extrapolate these previous findings to the interactions occurring in full-length Munc13-4. Using clear-native gel electrophoresis, Boswell *et al.* suggested that Munc13-4 might dimerize (62). Our data (Fig. 6) are the only direct, hydrodynamic analysis of full-length Munc13-4, and although they are strongly consistent with monomeric Munc13-4 as the dominant state under our solution conditions, higher oligomers may be possible at increased protein concentrations or in a crowded microenvironment, such as might occur at sites of fusion. Constraining Munc13-4 to span between plasma and vesicle membranes might increase its effective concentration to the point where multimerization could occur. This will need to be evaluated in future biophysical studies.

Our results imply a potential Ca^{2+} sensing role for Munc13-4 in platelets, that is, perhaps, downstream of granule docking. Our data are consistent with divergent roles for the two C2 domains of Munc13-4, specifically relevant to their Ca^{2+} binding. Several other C2-domain-containing proteins have also been detected in platelets (*i.e.*, Slp4, DOC2, and synaptotagmin (28, 29, 66)), thus there are potential Ca^{2+} sensors which could affect secretion. It is interesting to note that many proteins with 2 C2 domains show distinct roles for each. For example, a Ca^{2+}-binding role for the C2B domains of synaptotagmins has been shown to be important for neuronal secretion (39, 67, 68). At this stage it is naïve to claim that Munc13-4 is the only relevant Ca^{2+} sensor for platelet exocytosis. However, our data do point to two intriguing aspects of Munc13-4's role in dense granule release that show it contributes to the activation of platelet secretion. First, Munc13-4 is important for granule immobilization/tethering even in resting platelets. Given the low intra-platelet concentrations of free Ca^{2+}, one would assume that this tethering function is not completely Ca^{2+}-dependent. Second, upon stimulation, which includes an increase in intra-platelet Ca^{2+}, the tethered granules fuse and their cargo is released. No significant release of dense granule cargo (mepacrine) is seen in the absence of Munc13-4. This could be simply due to the lack of tethered granules or because Munc13-4 performs a second, Ca^{2+}-dependent process that is important for SNARE-mediated fusion. C2 domains in other proteins have been shown to insert into bilayers presumably to promote membrane fusion (69, 70). At this stage, our experiments do not differentiate these two possibilities. What our data do demonstrate is that Munc13-4 juxtaposes vesicle membranes, stabilizes granules before and during platelet secretion, and stimulates membrane fusion in response to Ca^{2+} suggesting that Munc13-4 could contribute to a calcium response that activates granule release. This is essential for the rapid release of paracrine, dense granule cargo (*i.e.* ADP) and is thus critical for hemostasis.

Acknowledgments

We are also indebted to the members of the Whiteheart and Fried laboratories for their editorial comments during the preparation of this manuscript. This work is supported by NIH grants (HL56652 and HL082193) to S.W.W., a predoctoral fellowship from the Great Rivers Affiliate of the AHA (0615238B) to Q.R., and a postdoctoral fellowship from the Great Rivers Affiliate of the AHA (2240048) to M.C.C.

ABBREVIATIONS

	Soluble NSF Attachment Protein Receptor
SNAP-23	Synaptosomal Associated Protein-23
Unc	Uncoordinated
Munc	Mammalian Uncoordinated
VAMP	vesicle associated membrane protein
STXBP5	syntaxin binding protein 5
PS	phosphatidylserine
PC	phosphatidylcholine
NBD-PE	*N*-(7-nitro-2-1,3-benzoxadiazol-4-yl)-1,2-dipalmitoyl phosphatidyl-ethanolamine
Rhodamine-PE	*N*-(lissamine rhodamine B sulfonyl)-1,2-dipalmitoyl phosphatidylethanolamine
VWF	von Willebrand factor
PF4	platelet factor 4
HPS	Hermansky Pudlak Syndrome
GPS	Gray Platelet Syndrome (GPS)
FRET	fluorescence energy transfer
PCR	polymerase chain reaction
MSD	mean square displacement
GST	glutathione S transferase
AUC	analytical ultracentrifugation

References

1. Rendu F, Brohard-Bohn B. The platelet release reaction: granules' constituents, secretion and functions. Platelets. 2001; 12(5):261–73. [PubMed: 11487378]
2. Michelson, AD. Platelets. San Diego: Elsevier Science; 2002.
3. Huizing M, Anikster Y, Gahl WA. Hermansky-Pudlak syndrome and related disorders of organelle formation. Traffic. 2000; 1(11):823–35. [PubMed: 11208073]
4. White JG. Platelet granule disorders. Crit Rev Oncol Hematol. 1986; 4(4):337–77. [PubMed: 3513985]
5. Smith MP, Cramer EM, Savidge GF. Megakaryocytes and platelets in alpha-granule disorders. Baillieres Clin Haematol. 1997; 10(1):125–48. [PubMed: 9154319]
6. Nurden AT, Nurden P. The gray platelet syndrome: clinical spectrum of the disease. Blood Rev. 2007; 21(1):21–36. [PubMed: 16442192]

7. Huo Y, Schober A, Forlow SB, Smith DF, Hyman MC, Jung S, et al. Circulating activated platelets exacerbate atherosclerosis in mice deficient in apolipoprotein E. Nat Med. 2003; 9(1):61–7. [PubMed: 12483207]
8. Weber C. Platelets and chemokines in atherosclerosis: partners in crime. Circ Res. 2005; 96(6):612–6. [PubMed: 15802619]
9. Li Y, Woo V, Bose R. Platelet hyperactivity and abnormal Ca($^{2+}$) homeostasis in diabetes mellitus. Am J Physiol Heart Circ Physiol. 2001; 280(4):H1480–9. [PubMed: 11247757]
10. Vinik AI, Erbas T, Park TS, Nolan R, Pittenger GL. Platelet dysfunction in type 2 diabetes. Diabetes Care. 2001; 24(8):1476–85. [PubMed: 11473089]
11. Weber T, Zemelman BV, McNew JA, Westermann B, Gmachl M, Parlati F, et al. SNAREpins: Minimal Machinery for Membrane Fusion. Cell. 1998; 92:759–72. [PubMed: 9529252]
12. Rothman JE, Warren G. Implications of the SNARE hypothesis for intracellular membrane topology and dynamics. Cur Biol. 1994; 4:220–33.
13. Polgar J, Chung SH, Reed GL. Vesicle-associated membrane protein 3 (VAMP-3) and VAMP-8 are present in human platelets and are required for granule secretion. Blood. 2002; 100(3):1081–3. [PubMed: 12130530]
14. Chen D, Bernstein AM, Lemons PP, Whiteheart SW. Molecular mechanisms of platelet exocytosis: role of SNAP-23 and syntaxin 2 in dense core granule release. Blood. 2000; 95(3):921–9. [PubMed: 10648404]
15. Ren Q, Barber HK, Crawford GL, Karim ZA, Zhao C, Choi W, et al. Endobrevin/VAMP-8 is the primary v-SNARE for the platelet release reaction. Mol Biol Cell. 2007; 18(1):24–33. [PubMed: 17065550]
16. Flaumenhaft R, Croce K, Chen E, Furie B, Furie BC. Proteins of the exocytotic core complex mediate platelet alpha-granule secretion. Roles Of vesicle-associated membrane protein, snap-23, and syntaxin 4. J Biol Chem. 1999; 274:2492–501. [PubMed: 9891020]
17. Ye S, Karim ZA, Al Hawas R, Pessin JE, Filipovich AH, Whiteheart SW. Syntaxin-11, but not syntaxin-2 or syntaxin-4, is required for platelet secretion. Blood. 2012; 120(12):2484–92. [PubMed: 22767500]
18. Golebiewska EM, Harper MT, Williams CM, Savage JS, Goggs R, Fischer von Mollard G, et al. Syntaxin 8 regulates platelet dense granule secretion, aggregation, and thrombus stability. J Biol Chem. 2015; 290(3):1536–45. [PubMed: 25404741]
19. Koseoglu S, Peters CG, Fitch-Tewfik JL, Aisiku O, Danglot L, Galli T, et al. VAMP-7 links granule exocytosis to actin reorganization during platelet activation. Blood. 2015; 126(5):651–60. [PubMed: 25999457]
20. Houng A, Polgar J, Reed GL. Munc18-syntaxin complexes and exocytosis in human platelets. J Biol Chem. 2003; 278(22):19627–33. [PubMed: 12649283]
21. Al Hawas R, Ren Q, Ye S, Karim ZA, Filipovich AH, Whiteheart SW. Munc18b/STXBP2 is required for platelet secretion. Blood. 2012; 120(12):2493–500. [PubMed: 22791290]
22. Tolmachova T, Abrink M, Futter CE, Authi KS, Seabra MC. Rab27b regulates number and secretion of platelet dense granules. Proc Natl Acad Sci U S A. 2007; 104(14):5872–7. [PubMed: 17384153]
23. Ye S, Huang Y, Joshi S, Zhang J, Yang F, Zhang G, et al. Platelet secretion and hemostasis require syntaxin-binding protein STXBP5. J Clin Invest. 2014; 124(10):4517–28. [PubMed: 25244094]
24. Ren Q, Wimmer C, Chicka MC, Ye S, Ren Y, Hughson FM, et al. Munc13-4 is a limiting factor in the pathway required for platelet granule release and hemostasis. Blood. 2010; 116(6):869–77. [PubMed: 20435885]
25. Harper MT, van den Bosch MT, Hers I, Poole AW. Platelet dense granule secretion defects may obscure alpha-granule secretion mechanisms: evidence from Munc13-4-deficient platelets. Blood. 2015; 125(19):3034–6. [PubMed: 25953980]
26. Savage JS, Williams CM, Konopatskaya O, Hers I, Harper MT, Poole AW. Munc13-4 is critical for thrombosis through regulating release of ADP from platelets. J Thromb Haemost. 2013; 11(4): 771–5. [PubMed: 23331318]
27. Chapman ER. How Does Synaptotagmin Trigger Neurotransmitter Release? Annu Rev Biochem. 2008

28. Hampson A, O'Connor A, Smolenski A. Synaptotagmin-like protein 4 and Rab8 interact and increase dense granule release in platelets. J Thromb Haemost. 2013; 11(1):161–8.
29. Neumuller O, Hoffmeister M, Babica J, Prelle C, Gegenbauer K, Smolenski AP. Synaptotagmin-like protein 1 interacts with the GTPase-activating protein Rap1GAP2 and regulates dense granule secretion in platelets. Blood. 2009; 114(7):1396–404. [PubMed: 19528539]
30. Neeft M, Wieffer M, de Jong AS, Negroiu G, Metz CH, van Loon A, et al. Munc13-4 is an effector of rab27a and controls secretion of lysosomes in hematopoietic cells. Mol Biol Cell. 2005; 16(2): 731–41. [PubMed: 15548590]
31. Crozat K, Hoebe K, Ugolini S, Hong NA, Janssen E, Rutschmann S, et al. Jinx, an MCMV susceptibility phenotype caused by disruption of Unc13d: a mouse model of type 3 familial hemophagocytic lymphohistiocytosis. J Exp Med. 2007; 204(4):853–63. [PubMed: 17420270]
32. Feldmann J, Callebaut I, Raposo G, Certain S, Bacq D, Dumont C, et al. Munc13-4 is essential for cytolytic granules fusion and is mutated in a form of familial hemophagocytic lymphohistiocytosis (FHL3). Cell. 2003; 115(4):461–73. [PubMed: 14622600]
33. Shirakawa R, Higashi T, Tabuchi A, Yoshioka A, Nishioka H, Fukuda M, et al. Munc13-4 is a GTP-Rab27-binding protein regulating dense core granule secretion in platelets. J Biol Chem. 2004; 279(11):10730–7. [PubMed: 14699162]
34. Pivot-Pajot C, Varoqueaux F, de Saint Basile G, Bourgoin SG. Munc13-4 regulates granule secretion in human neutrophils. J Immunol. 2008; 180(10):6786–97. [PubMed: 18453599]
35. Elstak ED, Neeft M, Nehme NT, Voortman J, Cheung M, Goodarzifard M, et al. The munc13-4-rab27 complex is specifically required for tethering secretory lysosomes at the plasma membrane. Blood. 2011; 118(6):1570–8. [PubMed: 21693760]
36. Johnson JL, Hong H, Monfregola J, Kiosses WB, Catz SD. Munc13-4 restricts motility of Rab27a-expressing vesicles to facilitate lipopolysaccharide-induced priming of exocytosis in neutrophils. J Biol Chem. 2011; 286(7):5647–56. [PubMed: 21148308]
37. Tucker WC, Weber T, Chapman ER. Reconstitution of Ca^{2+}-regulated membrane fusion by synaptotagmin and SNAREs. Science. 2004; 304(5669):435–8. [PubMed: 15044754]
38. Chicka MC, Hui E, Liu H, Chapman ER. Synaptotagmin arrests the SNARE complex before triggering fast, efficient membrane fusion in response to Ca^{2+} Nat Struct Mol Biol. 2008; 15(8): 827–35. [PubMed: 18622390]
39. Bhalla A, Chicka MC, Chapman ER. Analysis of the synaptotagmin family during reconstituted membrane fusion. Uncovering a class of inhibitory isoforms. J Biol Chem. 2008; 283(31):21799–807. [PubMed: 18508778]
40. Brown PH, Schuck P. Macromolecular size-and-shape distributions by sedimentation velocity analytical ultracentrifugation. Biophys J. 2006; 90(12):4651–61. [PubMed: 16565040]
41. Schuck P. On computational approaches for size-and-shape distributions from sedimentation velocity analytical ultracentrifugation. Eur Biophys J. 2010; 39(8):1261–75. [PubMed: 19806353]
42. Laue, TM., Shah, BD., Ridgeway, TM., Pelletier, SL. Computer-Aided Interpretation of Analytical Sedimentation Data For Proteins. In: Harding, SE.Rowe, AJ., Horton, JC., editors. Analytical Ultracentrifugation in Biochemistry and Polymer Science. Cambridge, England: The Royal Society of Chemistry; 1992. p. 90-125.
43. Ge S, Wittenberg NJ, Haynes CL. Quantitative and real-time detection of secretion of chemical messengers from individual platelets. Biochemistry. 2008; 47(27):7020–4. [PubMed: 18557631]
44. Jonnalagadda D, Sunkara M, Morris AJ, Whiteheart SW. Granule-mediated release of sphingosine-1-phosphate by activated platelets. Biochim Biophys Acta. 2014; 1841(11):1581–9. [PubMed: 25158625]
45. Weber T, Parlati F, McNew JA, Johnston RJ, Westermann B, Sollner TH, et al. SNAREpins are functionally resistant to disruption by NSF and alphaSNAP. J Cell Biol. 2000; 149(5):1063–72. [PubMed: 10831610]
46. Hellewell AL, Foresti O, Gover N, Porter MY, Hewitt EW. Analysis of familial hemophagocytic lymphohistiocytosis type 4 (FHL-4) mutant proteins reveals that S-acylation is required for the function of syntaxin 11 in natural killer cells. PloS one. 2014; 9(6):e98900. [PubMed: 24910990]

47. Nalefski EA, Wisner MA, Chen JZ, Sprang SR, Fukuda M, Mikoshiba K, et al. C2 domains from different Ca^{2+} signaling pathways display functional and mechanistic diversity. Biochemistry. 2001; 40(10):3089–100. [PubMed: 11258923]
48. Nalefski EA, Newton AC. Membrane binding kinetics of protein kinase C betaII mediated by the C2 domain. Biochemistry. 2001; 40(44):13216–29. [PubMed: 11683630]
49. McNew JA, Parlati F, Fukuda R, Johnston RJ, Paz K, Paumet F, et al. Compartmental specificity of cellular membrane fusion encoded in SNARE proteins. Nature. 2000; 407(6801):153–9. [PubMed: 11001046]
50. Balbo, A., Schuck, P. Analytical Ultracentrifugation in the Study of Protein Self-Association and Heterogeneous Protein-Protein Interactions. In: Golemis, E., Adams, PD., editors. Protein-Protein Interactions: A Molecular Cloning Manual Cold Spring Harbor. NY: Cold Spring Harbor Press; 2005. p. 253-77.
51. Dam J, Schuck P. Calculating sedimentation coefficient distributions by direct modeling of sedimentation velocity concentration profiles. Methods Enzymol. 2004; 384:185–212. [PubMed: 15081688]
52. García de la Torre J. Hydration from hydrodynamics. General considerations and applications of bead modelling to globular proteins. Biophys Chem. 2001; 93:159–70. [PubMed: 11804723]
53. Perkins SJ. X-ray and neutron scattering analyses of hydration shells: a molecular interpretation based on sequence predictions and modelling fits. Biophys Chem. 2001; 93:129–39. [PubMed: 11804721]
54. Skaer RJ, Flemans RJ, McQuilkan S. Mepacrine stains the dense bodies of human platelets and not platelet lysosomes. Br J Haematol. 1981; 49(3):435–8. [PubMed: 6170308]
55. Graham GJ, Ren Q, Dilks JR, Blair P, Whiteheart SW, Flaumenhaft R. Endobrevin/VAMP-8-dependent dense granule release mediates thrombus formation in vivo. Blood. 2009; 114(5):1083–90. [PubMed: 19395672]
56. Meng R, Wu J, Harper DC, Wang Y, Kowalska MA, Abrams CS, et al. Defective release of alpha granule and lysosome contents from platelets in mouse Hermansky-Pudlak syndrome models. Blood. 2015; 125(10):1623–32. [PubMed: 25477496]
57. Dudenhoffer-Pfeifer M, Schirra C, Pattu V, Halimani M, Maier-Peuschel M, Marshall MR, et al. Different Munc13 isoforms function as priming factors in lytic granule release from murine cytotoxic T lymphocytes. Traffic. 2013; 14(7):798–809. [PubMed: 23590328]
58. Schumacher D, Strilic B, Sivaraj KK, Wettschureck N, Offermanns S. Platelet-derived nucleotides promote tumor-cell transendothelial migration and metastasis via P2Y2 receptor. Cancer Cell. 2013; 24(1):130–7. [PubMed: 23810565]
59. Stegner D, Deppermann C, Kraft P, Morowski M, Kleinschnitz C, Stoll G, et al. Munc13-4-mediated secretion is essential for infarct progression but not intracranial hemostasis in acute stroke. J Thromb Haemost. 2013; 11(7):1430–3. [PubMed: 23659589]
60. Zhang K, Jordan MB, Marsh RA, Johnson JA, Kissell D, Meller J, et al. Hypomorphic mutations in PRF1, MUNC13-4, and STXBP2 are associated with adult-onset familial HLH. Blood. 2011; 118(22):5794–8. [PubMed: 21881043]
61. Zur Stadt U, Beutel K, Kolberg S, Schneppenheim R, Kabisch H, Janka G, et al. Mutation spectrum in children with primary hemophagocytic lymphohistiocytosis: molecular and functional analyses of PRF1, UNC13D, STX11, and RAB27A. Hum Mutat. 2006; 27(1):62–8. [PubMed: 16278825]
62. Boswell KL, James DJ, Esquibel JM, Bruinsma S, Shirakawa R, Horiuchi H, et al. Munc13-4 reconstitutes calcium-dependent SNARE-mediated membrane fusion. J Cell Biol. 2012; 197(2): 301–12. [PubMed: 22508512]
63. Fukuda M. Rab27 effectors, pleiotropic regulators in secretory pathways. Traffic. 2013; 14(9):949–63. [PubMed: 23678941]
64. Ma C, Hou H, Tian W, Xu T. Expression, purification and characterization of critical domains of Munc13-1. Acta Biochim Biophys Sin (Shanghai). 2007; 39(8):617–23. [PubMed: 17687497]
65. Lu J, Machius M, Dulubova I, Dai H, Sudhof TC, Tomchick DR, et al. Structural basis for a Munc13-1 homodimer to Munc13-1/RIM heterodimer switch. PLoS Biol. 2006; 4(7):e192. [PubMed: 16732694]

66. Burkhart JM, Vaudel M, Gambaryan S, Radau S, Walter U, Martens L, et al. The first comprehensive and quantitative analysis of human platelet protein composition allows the comparative analysis of structural and functional pathways. Blood. 2012; 120(15):e73–82. [PubMed: 22869793]

67. Bhalla A, Tucker WC, Chapman ER. Synaptotagmin isoforms couple distinct ranges of Ca^{2+}, Ba^{2+}, and Sr^{2+} concentration to SNARE-mediated membrane fusion. Mol Biol Cell. 2005; 16(10): 4755–64. [PubMed: 16093350]

68. Gaffaney JD, Dunning FM, Wang Z, Hui E, Chapman ER. Synaptotagmin C2B domain regulates Ca^{2+}-triggered fusion in vitro: critical residues revealed by scanning alanine mutagenesis. J Biol Chem. 2008; 283(46):31763–75. [PubMed: 18784080]

69. Martens S, Kozlov MM, McMahon HT. How synaptotagmin promotes membrane fusion. Science. 2007; 316(5828):1205–8. [PubMed: 17478680]

70. Ward KE, Ropa JP, Adu-Gyamfi E, Stahelin RV. C2 domain membrane penetration by group IVA cytosolic phospholipase A(2) induces membrane curvature changes. J Lipid Res. 2012; 53(12): 2656–66. [PubMed: 22991194]

SUMMARY STATEMENT

Platelet exocytosis, mediated by SNAREs and Ca^{2+}-dependent regulators, is critical for hemostasis. Munc13-4 binds membranes in a Ca^{2+}- and PS-dependent manner and acts as a tethering factor for pre-docked platelet dense granule secretion to mediate rapid response to vascular damage. (40 words)

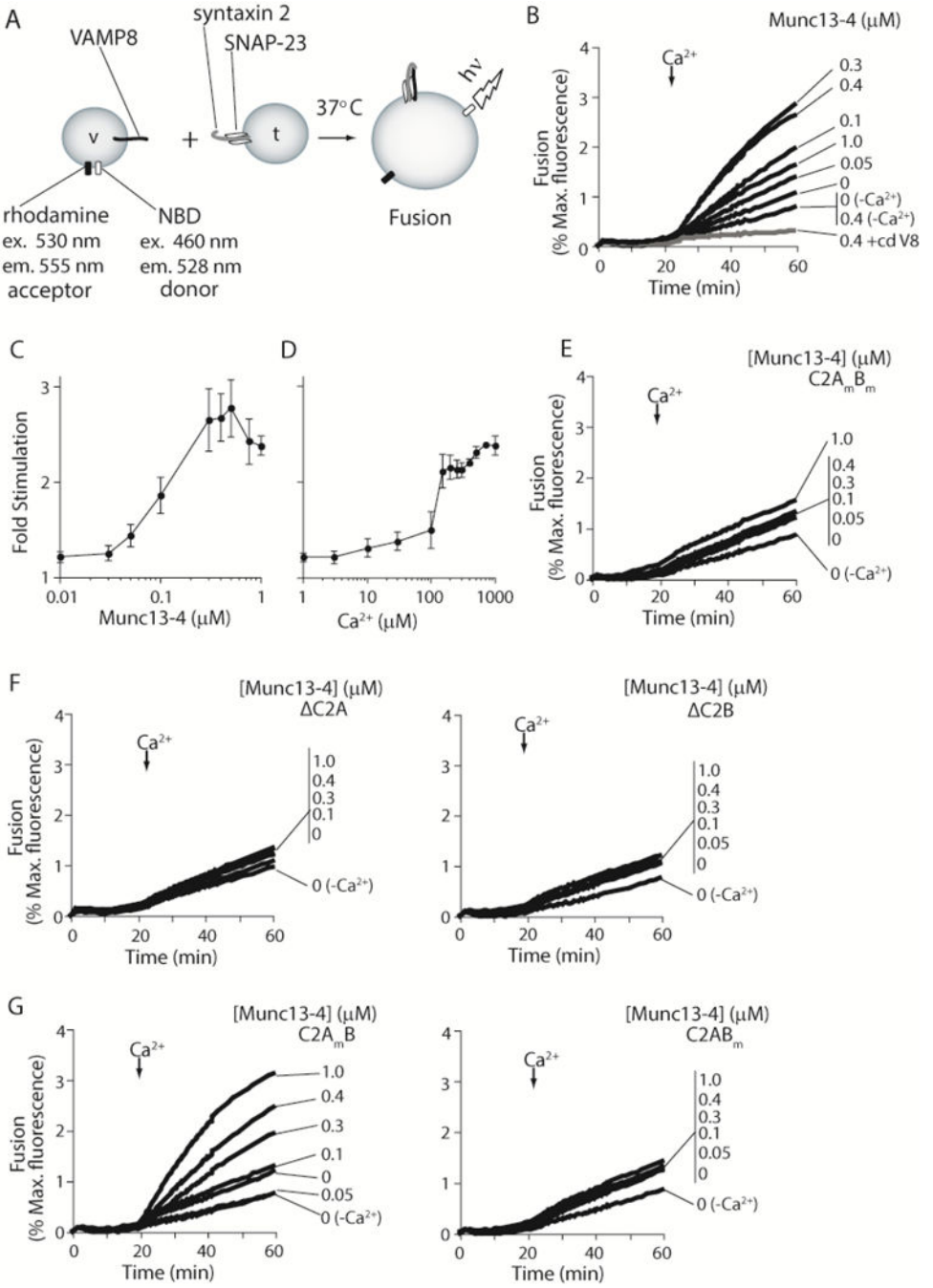

Figure 1. Munc13-4 Stimulates SNARE-mediated membrane fusion in response to Ca^{2+}

(A) Illustration depicting the *in vitro* reconstituted membrane fusion assay. Fusion of v-SNARE (VAMP8; v) vesicles containing a donor and acceptor FRET pair with unlabeled t-SNARE vesicles (syntaxin 2/SNAP-23; t) results in dilution of the FRET pair. Membrane fusion is measured as an increase in donor fluorescence over time. **(B)** Reconstituted membrane fusion assays were carried out using a 1:1 t:v-SNARE vesicle ratio. Recombinant Munc13-4 was added as indicated. Reactions were carried out in 0.2 mM EGTA. Ca^{2+} was added to a final concentration of 1 mM at t = 20 min. Samples lacking Ca^{2+}-addition

(−Ca^{2+}) were also included. As a control, the cytoplasmic domain of VAMP8 (+cdV8, 10 μM) was added to inhibit SNARE-mediated fusion (gray line). Fusion was monitored for 60 min at 37°C, normalized to the maximum donor fluorescence signal (% Max. fluorescence), and plotted as a function of time. **(C)** The final extent of fusion at each Munc13-4 concentration tested in panel B was normalized to the final extent of fusion obtained in samples lacking Munc13-4 (Fold Stimulation) and plotted as a function of Munc13-4 concentration. **(D)** Fusion reactions containing 0.4 μM Munc13-4 were carried out as in panel B. The final concentration of Ca^{2+} added at t=20 min was varied from 1 μM to 1 mM. The final extent of fusion was normalized as in *B* and plotted as a function of the Ca^{2+} concentration. **(E)** Fusion reactions were carried out as in panel B using recombinant Munc13-4 in which the Ca^{2+}-coordinating aspartic acid residues in the C2 domains were substituted with asparagine residues. Error bars represent the standard error from n≥3. **(F)** Experiments were repeated using recombinant Munc13-4 lacking the Ca^{2+}-coordinating C2A (ΔC2A, left panel) or C2B (ΔC2B, right panel) domain. Data are representative of n>3. **(G)** Experiments were repeated using recombinant Munc13-4 in which the Ca^{2+}-coordinating aspartic acid residues in the C2A ($C2A_mB$, left panel) or C2B ($C2AB_m$, right panel) were substituted with asparagine residues ($C2A_mB$ = D127N, D133N, D206N, D208N, D241N; $C2AB_m$ = D941N, D947N, D1005N, D1007N, D1013N). Data are representative of n≥3.

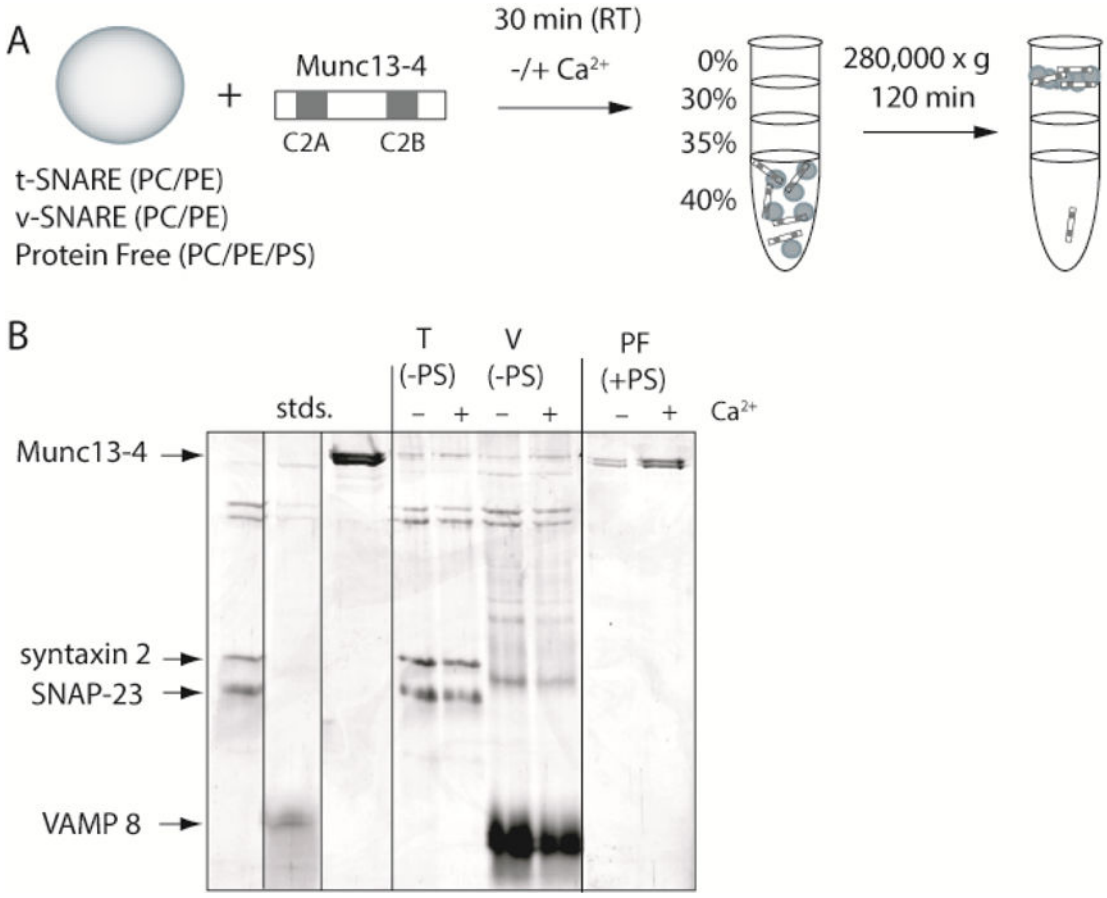

Figure 2. Munc13-4 interacts with lipids, but not with SNAREs in a Ca^{2+}-dependent manner

(A) Diagram of the flotation assay used to monitor binding interactions (see also Materials and Methods). Recombinant Munc13-4 (2.0 μM) was incubated with either t-SNARE vesicles harboring SNAP-23 and Syntaxin 2 (**T**), v-SNARE vesicles harboring VAMP8 (**V**), or protein free vesicles (**PF**) containing PS for 30 min at room temperature in the absence or presence of Ca^{2+} (1 mM). The lipid composition of the protein free vesicles was 40% PC, 30% PE and 30% PS. The lipid composition of the t- and v-SNARE vesicles was 70% PC and 30% PE. Note: the t- and v-SNARE vesicles did not contain PS. Reactions were layered with decreasing concentrations of Accudenz buffer and subjected to centrifugation. Vesicles, and any components bound to the vesicles, floated to the 0%–30% Accudenz interface, were collected, and analyzed by SDS-PAGE. Unbound protein remained in the lower layers. **(B)** SDS-PAGE analysis of the floatation experiment diagramed in panel A. Proteins were visualized by staining with Coomassie blue. Gel is representative of n≥3.

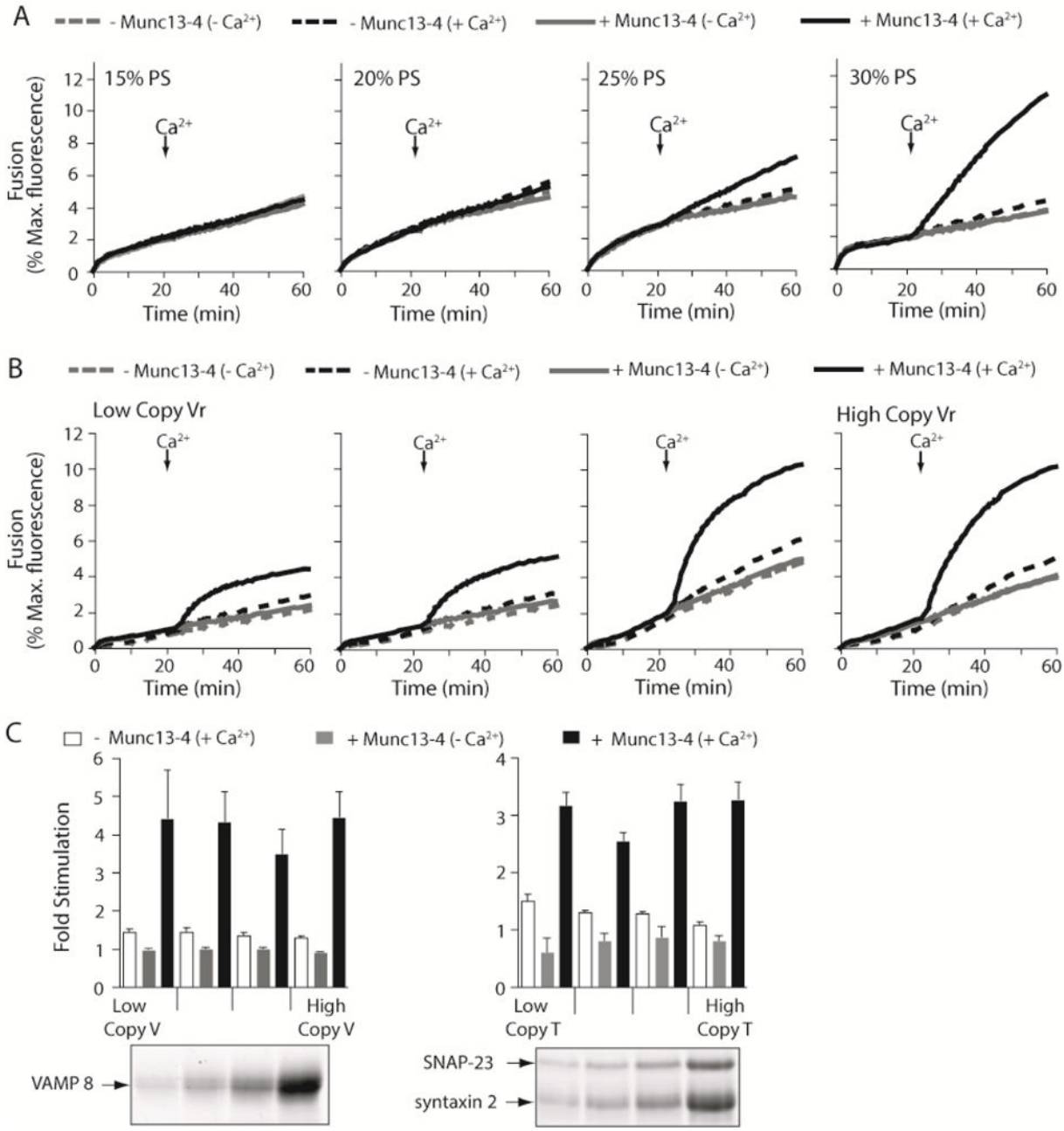

Figure 3. Ca^{2+}-Munc13-4 stimulated fusion is dependent upon the PS concentration of vesicles, but not on SNARE copy number

Reconstituted membrane fusion assays were carried out as described in Figure 1 **(A)** 0.4 μM Munc13-4 was added to reactions as indicated and t- and v-SNARE vesicles harboring increasing concentrations of PS were used. PC concentrations were adjusted to accommodate the increase in PS concentration. Traces are representative from n≥3. **(B)** Membrane fusion assays were carried out using v-SNARE vesicles with increasing copy numbers of VAMP8; t-SNARE vesicles remained unchanged and were the same as described in Figure 1. Vesicles harbored 30% PS. **(C)** (left) Data from panel B were normalized as described in Figure 1C and plotted as Fold Stimulation above – Munc13-4 (-Ca^{2+}). Error

bars represent the standard error from n≥3. (right) Experiments in panel B were repeated using t-SNARE vesicles with increasing copy numbers of syntaxin 2-SNAP-23 heterodimer and plotted as described previously; v-SNARE vesicles remained unchanged and were the same as described in Figure 1. (lower panels) Equal amounts of low, intermediate, and high copy v-SNARE and t-SNARE vesicles were analyzed by SDS-PAGE followed by staining with Coomassie blue.

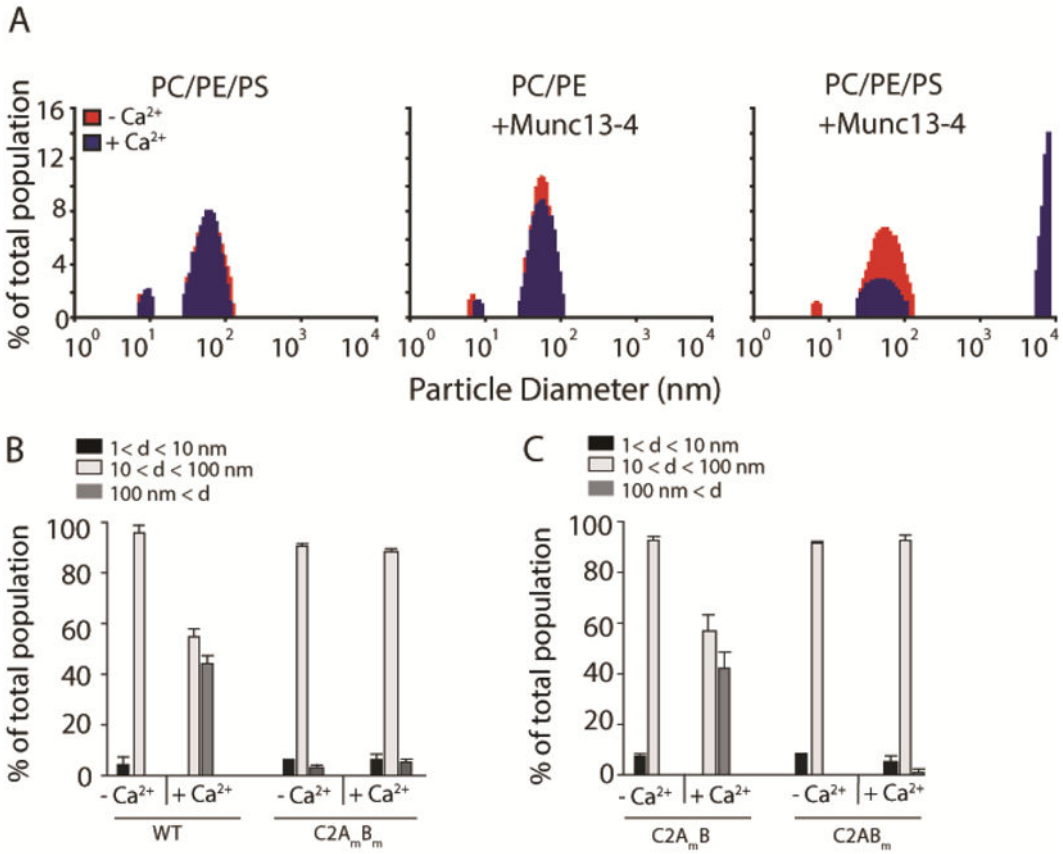

Figure 4. PS-containing vesicles form large aggregates in the presence of Ca^{2+}-Munc13-4

(A) Protein free vesicles comprising 40% PC/30% PE/30% PS (PC/PE/PS) or 70% PC/30% PE (PC/PE) were mixed with buffer in a cuvette that was placed into the chamber of a DynaPro 99 instrument pre-heated to 37°C. Ca^{2+} (1 mM) was added to reactions after measurements stabilized (~ 1 min). The size distribution of particles within the cuvette was measured prior to (red) and after (blue) Ca^{2+} addition and plotted as a histogram. Munc13-4 (0.3 μM) was included in reactions as indicated. Conditions mimicked the conditions used for in vitro membrane fusion assays. (left) Both before and after Ca^{2+} addition, vesicles harboring PS exist as individual particles sized mainly between 80 and 100 nm. (middle) In reactions including Munc13-4, vesicles lacking PS exist as individual particles sized mainly between 80 and 100 nm both before and after Ca^{2+} addition. (right) In reactions including Munc13-4, PS-harboring vesicles exist as individual particles sized mainly between 80 and 100 nm before Ca^{2+} addition, but following Ca^{2+}-addition, the fraction of PS-harboring vesicles that exist as individual particles decreases and large vesicle aggregates form with sizes exceeding 10 μm. **(B)** Data from panel A were grouped into three categories: particles with diameters less than 10 nm (black), 10 nm to 100 nm (white), and greater than 100 nm (gray). The fraction of particles within each group (% total population) was plotted for reactions prior to and after Ca^{2+} addition. Experiments were repeated using recombinant Munc13-4 in which the Ca^{2+}-coordinating aspartic acid residues in the C2A and C2B domains were substituted with asparagine residues ($C2A_mB_m$). Data are representative from n≥3. **(C)** Experiments were repeated using recombinant Munc13-4 in which the Ca^{2+}-

coordinating aspartic acid residues in only the C2A ($C2A_mB$) or C2B ($C2AB_m$) domain were substituted with asparagine residues. Data are representative of n≥3.

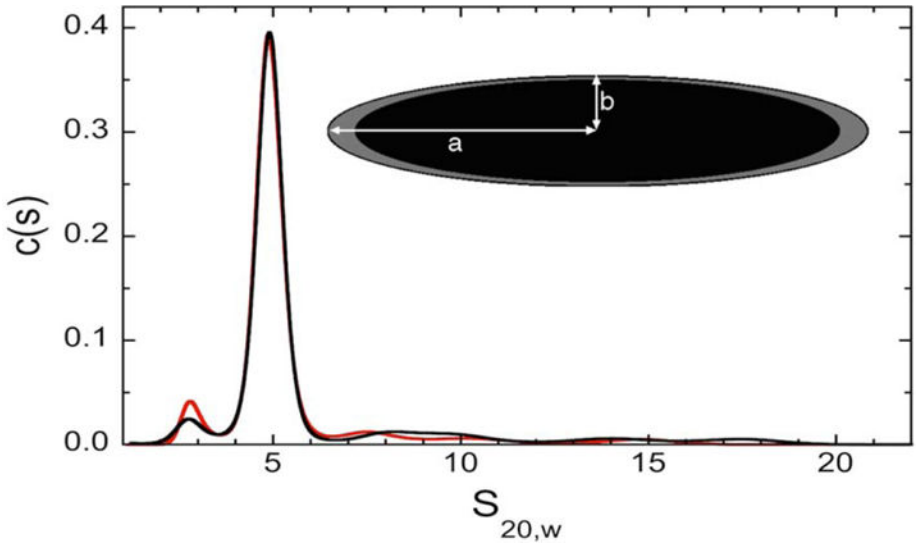

Figure 5. Sedimentation velocity analysis of Munc13-4 proteins

Measurements were made in Ca^{2+}-buffer (red curve) and EGTA-buffer (black curve). C(s) distributions were calculated using the program SEDFIT. Translational frictional ratios, $f/f_{0,}$ were calculated with SEDNTERP, using mean $s_{20,w}$ values of the major species as input. Frictional ratios were used to estimate the dimensions of hydrodynamically-equivalent prolate ellipsoids, using the $\overline{\nu}$ method implemented in SEDNTERP and a hydration value of 0.3g/g-protein. (inset) The black ellipsoid shows the proportions of the protein alone, and the grey shell shows the extent to which this degree of hydration changes the dimensions of semi-major (a) and semi-minor (b) radii.

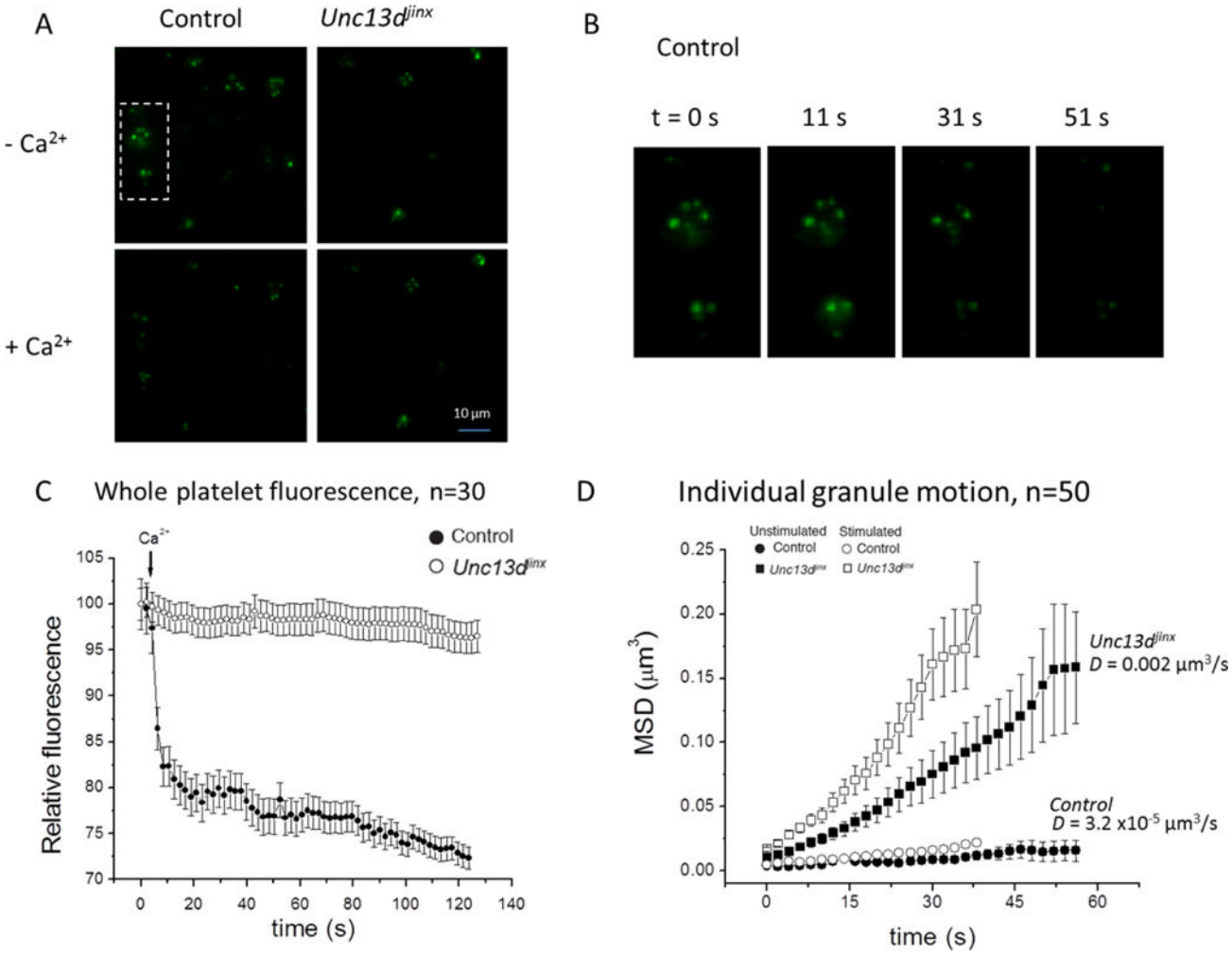

Figure 6. Munc13-4 stabilizes dense granules in platelets before and after the Ca^{2+} trigger

(A) Images of fields showing fluorescent-labeled dense granules in platelets from control and *Unc13d*^{Jinx} mice before (pre-Ca^{2+}) and after (post-Ca^{2+}) stimulation using the ionophore A23187. The box encases two control platelets shown in panel B. **(B)** Images of control platelets from panel A at t=0, 11, 31, and 51 sec. **(C)** The relative fluorescence intensity of whole platelets from control (●) or *Unc13d*^{Jinx} (○) mice was plotted versus time, following stimulation with 0.7 mM Ca^{2+} and A23187 (1 µM) at t=0 sec. Data represent the mean −/+ SEM for n=30 platelets. **(D)** Individual granules in platelets from control (●,○) and *Unc13d*^{Jinx} (■,□) mice were tracked over time on the basis of their center of intensity, in three dimensions. The mean-squared displacement of 50 granules was calculated and plotted versus time in unstimulated samples(●, ■) or samples stimulated with 0.7 mM Ca^{2+} and A23187 (1 µM; ○, □) at t=0 sec. The average mean-squared displacement *D* of the control and *Unc13d*^{Jinx} samples is indicated on the graph. Error bars represent SEM. We note that data for the stimulated condition was collected for only 40 sec because most granule secretion from control platelets was completed by this time.